Perception, 1985, volume 14, pages 225-238

Sensitivity to shearing and compressive motion in random dots

Ken Nakayama, Gerald H Silverman
Smith-Kettlewell Institute of Visual Sciences, Medical Research Institute, San Francisco, CA 94115, USA
Donald I A MacLeod, Jeffrey Mulligan
Department of Psychology, University of California at San Diego, La Jolla, CA 92093, USA
Received 20 February 1984, in revised form 15 May 1984

Abstract. The sensitivity of the visual system to motion of differentially moving random dots was measured. Two kinds of one-dimensional motion were compared: standing-wave patterns where dot movement amplitude varied as a sinusoidal function of position along the axis of dot movement (longitudinal or compressional waves) and patterns of motion where dot movement amplitude varied as a sinusoidal function orthogonal to the axis of motion (transverse or shearing waves). Spatial frequency, temporal frequency, and orientation of the motion were varied. The major finding was a much larger threshold rise for shear than for compression when motion spatial frequency increased beyond 1 cycle deg^{-1}. Control experiments ruled out the extraneous cues of local luminance or local dot density. No conspicuous low spatial-frequency rise in thresholds for any type of differential motion was seen at the lowest spatial frequencies tested, and no difference was seen between horizontal and vertical motion. The results suggest that at the motion threshold spatial integration is greatest in a direction orthogonal to the direction of motion, a view consistent with elongated receptive fields most sensitive to motion orthogonal to their major axis.

1 Introduction

Moving random dots have been widely used in the study of human motion sensitivity (Julesz 1971; Braddick 1974; Lappin and Bell 1976; Nakayama and Tyler 1981). Such stimuli have two advantages.

First, a dense array of random dots is practically devoid of codable position cues and thus provides a psychophysical technique for examining early motion processing in isolation. This point was made by Nakayama and Tyler (1981) who argued that, because random patterns look indistinguishably random after substantial relative displacement of their elements (see Attneave 1954; Barlow 1961), psychophysical measures of motion sensitivity employing these patterns could only be mediated by a motion-sensitive system. Using such patterns, Nakayama and Tyler (1981) established that the minimum motion thresholds are not mediated by the same system as that responsible for fine positional acuity adjustements, ie those mechanisms required for vernier and other static hyperacuity tasks. Sensitivity to very small relative motions has a very different spatial characteristic than does the sensitivity to small differences in relative position. As such, the use of random-dot patterns isolates motion sensitivity from the contaminating influences of fine position sensitivity.

A second advantage of random dots is that they are two-dimensional and essentially isotropic. This enables one to explore two-dimensional spatial characteristics of motion processing, an option precluded with the more commonly used one-dimensional stimuli such as drifting sine-wave gratings. In this paper, we exploit both advantages, providing information as to how motion information is integrated in two dimensions.

Our general approach is to measure the ability of the observers to sense motion when different regions of the random-dot pattern are moving at different velocities. Two general types of differential motion are considered: shearing (or transverse) and compression (or longitudinal) waves.

With shearing waves velocity varies as a sinusoidal function of position in a direction orthogonal to the local direction of motion. Thus, for vertical shearing waves, the vertical movement of each point varies as a sinusoidal function of horizontal position and of time:

$$\Delta y = A\cos(2\pi f_s x)\cos(2\pi f_t t), \tag{1}$$

whereas for horizontal shearing motion the velocity of each point varies as a sinusoidal function of vertical position and of time:

$$\Delta x = A\cos(2\pi f_s y)\cos(2\pi f_t t); \tag{2}$$

Δx and Δy represent here the change in horizontal and vertical positions of a given visual point, f_s and f_t represent the spatial and temporal frequencies of the shearing wave, and A is the baseline-to-peak displacement.

Compression waves have a complementary characteristic: the velocity of each point varies in the direction of the local motion vector. Again, two orientations of such waves were employed, one using horizontal motion:

$$\Delta x = A\cos(2\pi f_s x)\cos(2\pi f_t t), \tag{3}$$

the other using vertical motion:

$$\Delta y = A\cos(2\pi f_s y)\cos(2\pi f_t t). \tag{4}$$

Examples of each type of differential motion having different orientations and spatial frequencies are depicted in figure 1. It should be noted that all moving patterns whose horizontal and vertical velocity components have Fourier transforms can be represented as a superposition of shearing and compression waves at different orientations, phases,

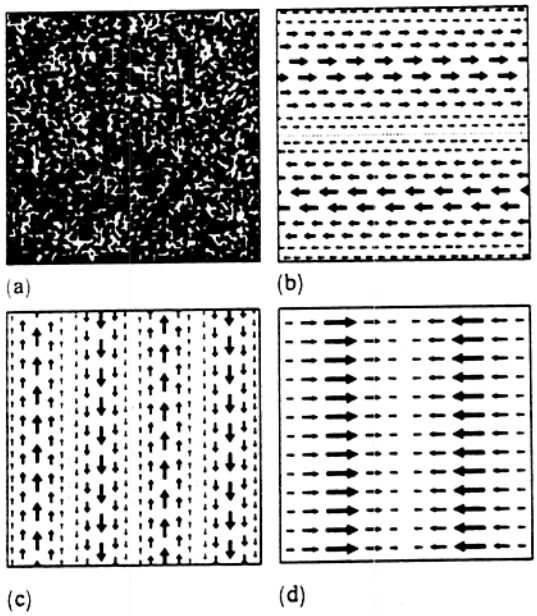

Figure 1. Schematic summary of some of the stimuli used in this study: (a) random-dot pattern generated in the frame of a CRT; (b) horizontal shearing (or transverse) motion (spatial frequency 1 cycle screen^{-1}); (c) vertical shearing motion (spatial frequency 2 cycles screen^{-1}); (d) horizontal compression motion (spatial frequency 1 cycle screen^{-1}).

Note that for shearing motion (b and c) the velocities (lengths of arrows) vary only in a direction orthogonal to the direction of motion, whereas for compression/rarefaction (d) they vary in the same direction as the motion. Arrows represent velocities for just one point in time in the sinusoidal temporal cycle. Thus the direction of each arrow is reversed one half period earlier or later.

and spatial frequencies (see Appendix 1). Therefore by measuring the sensitivity of the visual system to shearing and compressional waves we might expect to form a fairly-complete picture of its threshold sensitivity to moving patterns, at least to the extent that the motion sensing system can be regarded as approximately linear in its operation.

The major aim of this work was to measure the sensitivity of the visual system to these two types of differential motion, each at two different orientations. In each case we concentrated on the influence of spatial frequency (f_s) in order to reveal the two-dimensional spatial characteristics of motion processing.

2 Method

The procedure used to create random dots on a cathode ray oscilloscope has been described elsewhere (Nakayama and Tyler 1981; Nakayama 1981). In brief, a repeating binary noise sequence modulated the z axis, while synchronized to an $x-y$ raster scan. Unless otherwise specified, the square screen was viewed at a distance of 2.28 m and subtended 2.5 deg by 2.5 deg visual angle. Pixel size was 1.9 min visual angle and dark and light pixels were equiprobable. In any given experimental run, transverse or compression waves of motion were generated in either vertical or horizontal direction of motion. The observer's task was to adjust a log potentiometer so that the amplitude of motion was at threshold.

Shearing motion was imposed by electronically summing an AM-modulated sinusoidal signal with the fast raster sawtooth waveform, synchronized so that this sine-wave burst always began at the beginning of the slow raster sawtooth waveform. Compression waveforms were imposed by summing the same AM-modulated sinusoidal signal with the slow raster sawtooth.

Unless otherwise stated, all spatial-frequency tuning functions were obtained at the temporal frequency (f_t) of 2 Hz. This represents the frequency where motion sensitivity requires the minimum amplitude displacement (Tyler and Torres 1972; Nakayama and Tyler 1981). Space average luminance of the CRT display was about 15 cd m^{-2}; contrast was approximately 60%. Viewing was binocular.

3 Results

3.1 *Perceptual reciprocity between dot luminance and density*

With shear (transverse) waves, there is no expansion or contraction of dots per unit area (no divergence) and dot density remains constant. With compression waves, however, a special problem exists. Fluctuations in dot density are unavoidable as the dots locally converge or diverge. This raises the question as to whether compressional motion sensitivity can be isolated from the visual system's capacity to see local changes in dot density or changes in local luminance accompanying such changes in density. In other words, if one obtains a threshold for seeing differential motion in compression waves, it is essential to rule out the cue of dot density and/or luminance. To deal with this potential problem, we used a number of independent strategies. Our primary approach was to determine the capacity of the visual system to detect spatial nonuniformity in a random-dot pattern as we increased the static compression/rarefaction waveform amplitude. Thus we varied A in equation (3) and presented the resulting stimulus as a static pattern ($f_t = 0$). The observer's task was to detect the variation in density. We wanted to make sure that this threshold was much higher than the threshold for motion perception and thus would not contaminate the measurement of motion sensitivity. The relation between the peak-to-peak compressional amplitude thresholds for seeing this inhomogeneity and spatial frequency is plotted as the open circles in figure 2.

For very low frequencies, very large amounts of compressional displacement are necessary to see spatial inhomogeneity, whereas this decreases considerably as spatial

frequency increases. This decrease follows partly from the fact that, for a given compressional amplitude, dot-density variation (ρ) is proportional to spatial frequency (see Appendix 2):

$$\rho = 2\pi f_s A \cos(2\pi f_t t)\sin(2\pi f_s y). \tag{5}$$

Another way to view these data is to compare them with a line of constant-density modulation or contrast modulation (see diagonal line in figure 2). We found that the thresholds for seeing spatial inhomogeneity were about an order of magnitude higher than the ordinary contrast modulation transfer function (MTF) obtained with sinusoidal luminance gratings. These are comparable to MTFs obtained by others with density variations in random dots (van Meeteren and Barlow 1981).

Comparison of these thresholds with the compressional motion thresholds (look ahead to figure 4) shows that for very low spatial frequencies there is a large safety zone, consisting of an extended range of compressional displacements, which would remain invisible if viewed statically, although this becomes smaller for higher spatial frequencies. To have an even greater margin of security for measuring motion sensitivity in isolation, compensation for dot density by modulation of dot luminance was attempted.

We reasoned as follows. Suppose we controlled the luminance of each individual dot so that it was inversely proportional to local dot density. Would this compensation further reduce our ability to sense density inhomogeneities in random dots?

To answer this question, we used a second sinusoidal signal of the same frequency as the compressional waveform to modulate the luminance of the bright dots so that the luminance peak corresponded to where density was most reduced (see figure 3). Modulation of dot luminance was accomplished by a second AM signal generator phase-locked to the first AM generator with a phase lead of 90°. Only the bright pixels were luminance modulated; the 'floor' or equiprobable dark pixels remained at the same luminance.

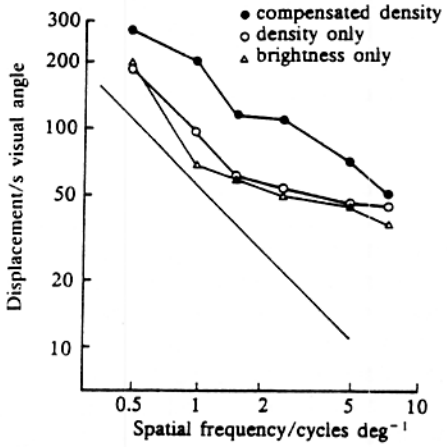

Figure 2. Control experiment to measure sensitivity to luminance or density variations in random dots. Open circles: threshold for seeing inhomogeneities in a static compressional/rarefacted displacement of random dots. Threshold peak-to-peak amplitude of the static compression is plotted as a function of spatial frequency. Each dot in the visual display is displaced vertically as a sinusoidal function of vertical position. Filled circles show the threshold for the same task with luminance compensation [see text and equations (5) and (6)]. Note that this curve is higher than the uncompensated one, and also note the degree to which one can effectively counteract changes in dot density with a compensatory modulation of dot luminance. Open triangles represent the threshold for seeing static differences in dot luminance modulation shown in terms of displacements which would lead to equivalent amounts of brightness modulation. The diagonal line represents a local space average luminance modulation of 5% for the experiment where either density alone is modulated or when luminance alone is modulated. Subject DIAM.

Having obtained the proper spatial-phase relationship between luminance and dot-density modulation for an arbitrary standard frequency of 1 cycle deg^{-1}, we then blurred the pattern with a diffusing screen and adjusted the amplitude of the brightness sinusoid relative to the displacement sinusoid so that it balanced the luminance modulation associated with the density change in random dots. From this we determined a coefficient of dot luminance (k) which provided the best cancellation of dot density at this standard spatial frequency. Because of the proportional relation between dot-density modulation and spatial frequency [as seen by equation (5)], we adjusted the compensatory luminance sinusoid amplitude (L) for all other spatial frequencies as follows:

$$L = kAf_s. \tag{6}$$

We then repeated the initial experiment, measuring the ability to see perceptual inhomogeneity in random dots *with* luminance compensation. To our surprise and satisfaction, such compensation raised density-modulation thresholds over almost the entire range of spatial frequencies examined (see filled circles of figure 2). So, despite the fact that individual dots are visible, variations in dot density can be effectively counteracted by variations in dot luminance, making patterns with reciprocal modulations of density and luminance perceptually uniform.

As a final observation in this series of experiments, we also measured the observer's ability to detect the brightness modulation of the dots when this was varied alone. As expected, luminance modulation thresholds, when plotted on the same metric, were the same as for density modulation, as can be seen from the open triangles in figure 2.

Aside from providing an important control for compressional movement, essentially eliminating variations in locally perceived brightness, the feasibility of substituting luminance for dot density despite the visibility of the dots suggests that total flux is integrated linearly, over a local retinal area, which is much larger than the area of a single pixel. Furthermore, the degree to which luminance can successfully compensate for dot density at a given spatial frequency (see difference between the upper curve in figure 2 and either of the two bottom curves) is an indication of the size of such linear summation units. The existence and nature of such linear summation units can be considered as a

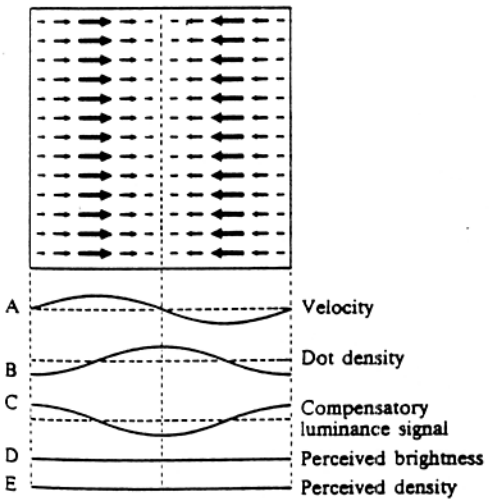

Figure 3. Pictorial description of the scheme to produce luminance compensation. A shows the profile of horizontal velocity, a function of horizontal position. B shows a corresponding profile of dot density, and C shows the compensatory luminance signal required to remove local variations in luminance. D and E represent the perceived uniformity of the field in terms of brightness and density, respectively. The figure does not show that velocity and dot density are in temporal as well as spatial quadrature.

separate subject distinct from motion sensitivity, however, and is being separately pursued (Mulligan and MacLeod 1984).

3.2 *Spatial frequency functions for compression and shear waves*

Having found an effective technique to minimize the cue of dot density by luminance compensation, we were in a favorable position to make our primary set of observations, the ability to see motion in shear and compression waves of different spatial frequencies. The basic results can be seen in figure 4. The open symbols show the change in differential shearing sensitivity as spatial frequency is varied. Note that for both horizontal and vertical shearing motion the curve is essentially the same, remaining flat between 0.1 and 1.0 cycle deg^{-1} and then rising rapidly as spatial frequency is increased. As such, the data confirm and extend the work of Nakayama and Tyler (1981).

The relation between compressional thresholds and spatial frequency is shown by the filled symbols. Although compressional motion thresholds also rise above 1 cycle deg^{-1}, they do so much more slowly. At 3 cycles deg^{-1}, for example, the threshold for compressional motion is one-half that for shear and this difference increases for even greater spatial frequencies. Also important to note is the lack of any systematic difference between vertical and horizontal compression waves.

The results for two other observers (KN and JS) were the same in all essential respects, showing the same quantitative difference between shear and compression waves at high frequencies, no difference at low spatial frequencies, and the lack of any differences between horizontal and vertical motion.

At this point it is important to describe the subjective characteristics of near-threshold motion above 2.5 cycles deg^{-1}. Instead of seeing the moving panels at the veridical-spatial frequency, observers often saw larger widths of coherently moving panels. This tendency was slightly more pronounced for compressional than for transverse motion.

A final point concerns the issue of dot density or local luminance, already mentioned as potential sources of contamination with regard to compressional thresholds. The dashed line on the top of figure 4 shows that the compensated static dot-density thresholds (taken from figure 2) are well above the thresholds obtained for compressional motion, exceeding them by a factor of 4. Thus, it is unlikely that the lower

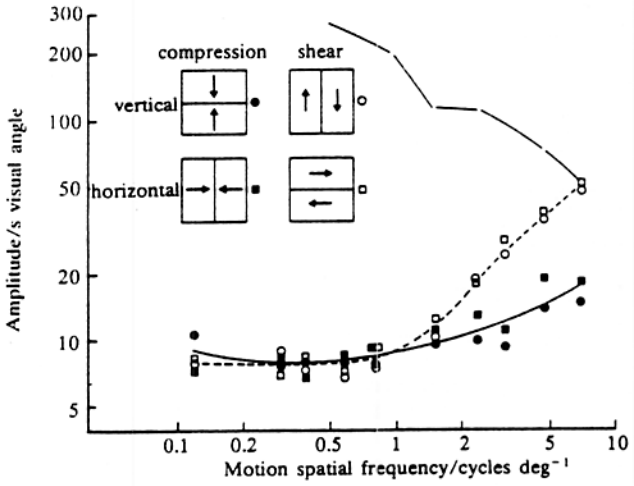

Figure 4. Spatial-frequency tuning characteristics of compression/rarefaction and shearing motion, each for horizontal and vertical motion. Lowest curve (solid symbols) shows the compressional thresholds, middle curve (open symbols) shows the shearing thresholds. Dashed upper curve shows the threshold for static dot 'inhomogeneity' with luminance compensation (taken from figure 2). Subject DIAM.

thresholds seen for compressional motion are determined by the sensitivity to static inhomogeneities.

3.3 *Temporal frequency*

Having obtained a clear-cut difference between compressional motion and shearing motion at higher spatial frequencies, we thought it instructive to compare the two in their dependence on temporal frequency. This provides a technique for determining whether a given set of displacements is mediated by a minimum velocity or position (Tyler and Torres 1972; Nakayama and Tyler 1978, 1981).

Should the system be sensitive to position or local density at the compressional motion threshold, one might expect that thresholds over a range of low temporal frequencies would be constant. Figure 5 shows that this is not the case. Threshold amplitude varies inversely with temporal frequency below 1 Hz (having a low-frequency slope of -1 in log–log coordinates), a relation established for shearing motion (Nakayama and Tyler 1981). This finding is in agreement with the view that compressional motion thresholds also require a minimum velocity rather than a minimum displacement. In this regard, both compressional and shearing motion appear to have the same temporal frequency characteristics, a result consistent with the view that they are mediated by the same velocity-sensitive mechanism.

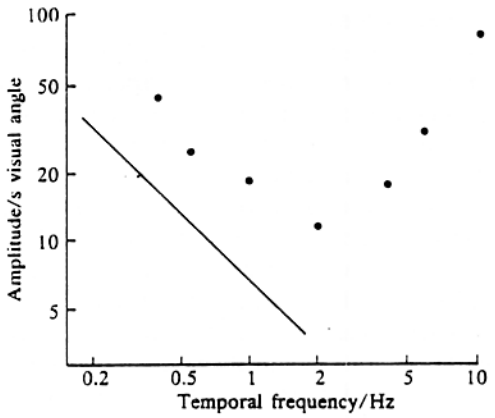

Figure 5. Temporal-frequency tuning function for compressional motion. Spatial frequency is 2.5 cycles deg^{-1}. Subject KN. Solid line represents a slope of -1, data parallel to this line indicate a sensitivity to a minimum velocity, not a minimum position.

3.4 *Trellis experiment*

Here we provide independent evidence for differences in sensitivity to compressional and shearing motion, using a stimulus which undergoes no change in dot density. In this experiment separate panels of random dots were demarcated by a 2 min visual angle thick 'trellis' of opaque bars placed in front of the screen. Each panel subtended a height of 10 min. In contrast to the previous experiment, motion within each panel was uniform, and thus represented a patch moving rigidly with no change in dot density. For the transverse case each panel moved as a rigid unit alternately to the right and then to the left. For compressional motion each alternate panel moved as a rigid unit but in the opposite vertical directions (see figure 6a). Without the trellis, compressional motion as defined above would have regions of perceptible dot overlap and dot separation. It is these otherwise visible changes in dot density that are effectively hidden behind the trellis. Figure 6b shows a twofold difference in threshold for the two different types of motion for two subjects, approximately the same difference as seen in figure 2 for the equivalent spatial frequency of 2.5 cycles deg^{-1}.

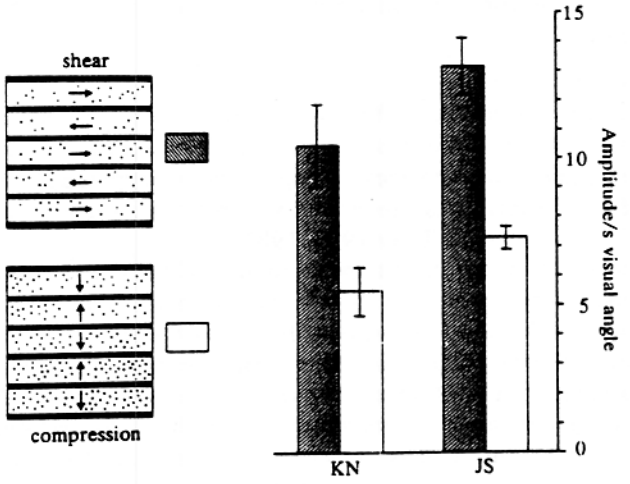

Figure 6. Trellis experiment. (a) Alternating panels with dots moving left and right (shearing) or down and up (compression). (b) The threshold for seeing shear and compression for two subjects.

3.5 *Counter-rolling cylinder experiment*

The technique of luminance-density compensation and the trellis experiment were introduced to deal with the problem of the spatial variation in dot luminance and dot density that arises during compressional motion. Separate and rather implausible objections could be raised against each of these control experiments because it could be argued neither completely eliminates artefactual cues that might disclose the presence of compressional motion. It could also be argued that in the trellis experiment partial occlusion of individual pixels at the boundaries of the occluding trellis might conceivably provide a cue, although this is very unlikely since each pixel will move about 2.5 to 3 s visual angle with respect to the trellis, a figure half the overall motion threshold and generally well below the vernier threshold. It could be also be argued that the luminance compensation experiment does not eliminate changes in pixel density but only minimizes their detectability. Changes in density are indeed inevitable when motion that is nonuniform (in the direction of the motion) is applied to an initially uniformly dense dot field. They can, however, be avoided by making the dot density initially nonuniform, with a spacing everywhere proportional to the velocity of the applied motion. When the motion stimulus is a spatial sinusoid, this means making the dot spacing (and pixel size) a sinusoidal function of position, with the same frequency and orientation and phase going to zero at the places where there is no applied motion. The resulting stimulus can most easily be imagined by picturing an array of contiguous rollers in a distant, frontoparallel plane, with a uniform random-dot texture on their surfaces (figure 7). Each roller represents half a cycle of our spatial sine wave. Dot spacing from the observer's standpoint follows the same sine wave (or more accurately, the full-wave rectified version of it shown in figure 7). When the rollers are set in motion, adjacent rollers rotate in opposite directions and the velocity is a sinusoidal function of position. The dot density at any fixed point in the observer's image of the rollers, however, is unaffected by the motion. It should also be mentioned that such a stimulus also removes the occlusion cue accompanying motion in the trellis experiment.

To produce a roller-like stimulus on a video display, we simply replaced the usual linear raster sawtooth with a waveform obtained by integrating the rectified sine wave of figure 7. The trace accelerates and decelerates sinusoidally, executing a stop of infinitesimal duration at each zero crossing of the sine wave; trace velocity, and hence pixel

size and spacing, are given by the rectified sine wave appropriate to the orthographic projection of a set of rollers. Motion is introduced in the usual way by adding the amplitude-modulated motion sinusoid to this modified raster waveform.

Despite the dissociation of density change and motion made possible by this stimulus, our results with it show detection thresholds similar both in their magnitude and in their spatial-frequency dependence to those of compressional motion seen in figure 4. This supports our assumption that the threshold differences between sinusoidal shear and compression are indeed motion thresholds and are unrelated to density or occlusion changes per se.

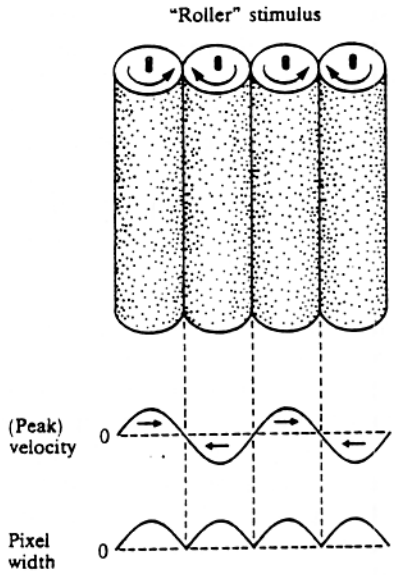

Figure 7. Counter-rolling 'rolling-pin' experiment: an electronic simulation of a set of rolling pins in which alternate pins rotate clockwise and anticlockwise, respectively, with a constant angular velocity, viewed from optical infinity. Note that the density of pixels and velocity vary accordingly.

4 Discussion

4.1 *Shear versus compression*

Our major finding is that there is a fundamental difference between the sensitivity to shear and that to compression waves. Because this difference is equally apparent for horizontal and vertical motion, it indicates that it is a spatial phenomenon defined with respect to the direction of motion and not due to any intrinsic difference between horizontal and vertical motion. The most prominent finding, of course, is the large difference between the two types of differential motion at high spatial frequencies. For shearing motion, sensitivity falls off rapidly as spatial frequency is increased, extending and confirming Nakayama and Tyler's (1981) results. For compression waves, however, sensitivity falls off much more slowly as spatial frequency is increased.

The fall-off function of shearing waves indicates the extent of spatial integration of movement information in the direction orthogonal to the motion, whereas the fall-off function for compression waves is indicative of spatial integration along the axis of motion. Looked at in this manner, it appears that spatial integration of movement information is highly anisotropic. Such results are consistent with the view that motion detecting units have elongated summation regions with a major axis orthogonal to the most sensitive or preferred direction of motion.

An elongated unit that is sensitive to motion immediately suggests the concept of the cortical receptive field as originally described by Hubel and Wiesel (1968). At this point,

however, it is possible to be more precise as to the meaning of an elongated receptive field. Consider the case where we have an elongated unit which sums luminance linearly over the receptive field. This is a formal restatement of Hubel and Wiesel's original idea of a simple cell where the response to a line was conceived as the sum of responses to individual spots, weighted by the sensitivity associated with each spot. Such a summation of luminance could provide the 'input' to a detector of motion. Cortical 'simple' cells are anisotropic in terms of luminance summation and could be best activated by patterns of light or dark aligned with the receptive field axis.

Would such a system explain our difference in results between high-frequency shear and compression waves? We think not. With random dots all configurations of dots within a local region are equally probable. This being the case, there are an equal number of situations where transverse motion can increase the linear alignment of bright dots with an 'on' receptive field as it would with a compressional motion of the same amplitude, and this is independent of spatial frequency. This being the case, we argue that the observed differences seen between shearing and compressional motion are not the result of an elongated luminance-summation mechanism but must be the result of spatial interaction at a higher level where directional selectivity is operative.

A more plausible model is similar to that of Barlow and Levick (1965) based on rabbit intraretinal recordings. In this instance, small subunits, capable of sensing motion only over a small distance, were hypothesized to pool their outputs to form a much larger, roughly circular, receptive field. Our results suggest first that the summation region is elongated rather than circular, and second that within the summation region the signals associated with areas moving in opposite directions can cancel or mutually inhibit one another. These assumptions are essential in order to account for the pronounced loss of sensitivity to high-frequency shearing motion.

4.2 *Limits of anisotropic spatial integration*

Although we have seen anisotropic spatial integration under all conditions described so far, it should be mentioned that it does not generalize to two additional experiments.

In the first of these we made measurements of the apparent velocity of suprathreshold moving shear patterns, matching the velocity to a field of uniformly moving random dots. In no cases did we see a decrease in apparent velocity for high-spatial-frequency shear patterns, indicating that the high-frequency fall-off in threshold seen for shear patterns applies only at the motion threshold and not at suprathreshold velocities. Such a difference between threshold and suprathreshold behavior could arise in several ways. For instance, it is conceivable that the very-small-amplitude motions at threshold are registered by a motion-sensitive system completely independent of the one that monitors the velocity of obviously moving objects. Or, alternatively, one could imagine that the insensitivity to high-frequency shear at threshold is the result of mutually inhibitory interactions between cells of opposite direction selectivity within an elongated region of the visual field, and that the inhibitory signals are relatively ineffective when the motion amplitude is high.

In the second experiment we examined differences in differentially moving thresholds for just two dots, either oscillating *along* the axis joining them (similar to compression) or oscillating at right angle to this axis (similar to shear). Distances between the dots were varied. No differences between these two curves were observed. It would seem that extended fields of either compression and shear waves are necessary for seeing differences between compression and shear. This is reasonable, since the spatially restricted two-dot motion field has a Fourier transform such that the greatest amplitudes occur at the lowest spatial frequencies, whatever the dot separation, making this stimulus unsuitable for demonstrating the differing spatial-frequency dependence of compression and shear sensitivity (Appendix 1). In the space domain the problem can be visualized by

considering two units with receptive fields offset so that only one of the pair of dots is a strong stimulus to them. Such a unit will be able to report the motion of that dot with little destructive effect of contrary motion by the other dot.

4.3 *Relation to previous work*

The present results confirm and extend the findings of Nakayama and Tyler (1981) who obtained a spatial-frequency function for horizontal transverse motion, one of the four functions reported here. Of interest is to compare our results with those of Rogers and Graham (1979, 1982a, 1982b, 1983) who employed similar random dot patterns and used them to study depth from motion rather than motion itself. Their threshold values were higher than ours, and they measured only two out of four functions. A major difference between their results and ours is a difference in sensitivity between shear and compression for stimuli of very low spatial frequency. An important difference between all of Rogers and Graham's experiments and our own may be the psychophysical criterion required. Our results are based on an observer's perception of motion and not depth. In one informal experiment we also used the criterion of depth when observing transverse motion at various spatial frequencies. Our results were in qualitative agreement with Rogers and Graham's, showing an upturn in sensitivity at very low spatial frequencies. As such, we attribute the major difference between their results and ours to the psychophysical criterion required.

Another point of comparison is the work of van Doorn and Koenderink (1982) whose results seem to be the reverse of our own. They measured signal-to-noise ratios for coherently moving random dots embedded in random noise, observing that transverse motion had lower threshold than compressional motion. Their experimental paradigm was sufficiently different from ours, however, to allow for the discrepancy. First, they worked at velocities far above the velocity threshold. Second, and as a consequence of the use of suprathreshold velocities, the experimental paradigm led to large differences in the 'lifetime' of the dot as it either moved a short distance across a differentially moving panel (as in the case of compressional motion) or a long distance along the same panel (as in the case of transverse motion). Because the lifetime has been shown to have considerable importance in motion processing (Lappin and Fuqua 1982; McKee 1982; Nakayama and Silverman 1984), stimuli affording longer lifetimes or dot existence would be more perceptible in terms of movement.

Regardless of the exact mechanism underlying anisotropic spatial integration, the results may have functional implications as to the coding of motion in general. Most important is the possible increase in signal-to-noise ratio if this process could extract the maximum amount of information from the visual scene by reducing redundant information (Barlow 1961). In any sufficiently small region of the visual field local motion is always orthogonal to moving contours. Signal strength (and signal-to-noise ratio) can be improved by integrating along the contour (orthogonal to the motion), but to integrate in the direction of the motion (so as to include regions where the moving contour is not present) is of no benefit.

Acknowledgements. This work was supported in part by grants 5P 30-EY 01186, EY 05408, 2SO7 RR 05566-16 from the National Institutes of Health, AFOSR 82-0345 from USAF, and The Smith-Kettlewell Eye Research Foundation. We wish to thank Graeme Mitchison for mathematical help with Appendix I and to Beatrice Golomb for comments on an earlier version of the manuscript.

References

Attneave F, 1954 "Some informational aspects of visual perception" *Psychological Review* **61** 183–193

Barlow H B, 1961 "Possible principles underlying the transformations of sensory messages" in *Sensory Communication* ed W A Rosenblith pp 217–234 (New York: John Wiley)

considering two units with receptive fields offset so that only one of the pair of dots is a strong stimulus to them. Such a unit will be able to report the motion of that dot with little destructive effect of contrary motion by the other dot.

4.3 *Relation to previous work*

The present results confirm and extend the findings of Nakayama and Tyler (1981) who obtained a spatial-frequency function for horizontal transverse motion, one of the four functions reported here. Of interest is to compare our results with those of Rogers and Graham (1979, 1982a, 1982b, 1983) who employed similar random dot patterns and used them to study depth from motion rather than motion itself. Their threshold values were higher than ours, and they measured only two out of four functions. A major difference between their results and ours is a difference in sensitivity between shear and compression for stimuli of very low spatial frequency. An important difference between all of Rogers and Graham's experiments and our own may be the psychophysical criterion required. Our results are based on an observer's perception of motion and not depth. In one informal experiment we also used the criterion of depth when observing transverse motion at various spatial frequencies. Our results were in qualitative agreement with Rogers and Graham's, showing an upturn in sensitivity at very low spatial frequencies. As such, we attribute the major difference between their results and ours to the psychophysical criterion required.

Another point of comparison is the work of van Doorn and Koenderink (1982) whose results seem to be the reverse of our own. They measured signal-to-noise ratios for coherently moving random dots embedded in random noise, observing that transverse motion had lower threshold than compressional motion. Their experimental paradigm was sufficiently different from ours, however, to allow for the discrepancy. First, they worked at velocities far above the velocity threshold. Second, and as a consequence of the use of suprathreshold velocities, the experimental paradigm led to large differences in the 'lifetime' of the dot as it either moved a short distance across a differentially moving panel (as in the case of compressional motion) or a long distance along the same panel (as in the case of transverse motion). Because the lifetime has been shown to have considerable importance in motion processing (Lappin and Fuqua 1982; McKee 1982; Nakayama and Silverman 1984), stimuli affording longer lifetimes or dot existence would be more perceptible in terms of movement.

Regardless of the exact mechanism underlying anisotropic spatial integration, the results may have functional implications as to the coding of motion in general. Most important is the possible increase in signal-to-noise ratio if this process could extract the maximum amount of information from the visual scene by reducing redundant information (Barlow 1961). In any sufficiently small region of the visual field local motion is always orthogonal to moving contours. Signal strength (and signal-to-noise ratio) can be improved by integrating along the contour (orthogonal to the motion), but to integrate in the direction of the motion (so as to include regions where the moving contour is not present) is of no benefit.

Acknowledgements. This work was supported in part by grants 5P 30-EY 01186, EY 05408, 2SO7 RR 05566-16 from the National Institutes of Health, AFOSR 82-0345 from USAF, and The Smith-Kettlewell Eye Research Foundation. We wish to thank Graeme Mitchison for mathematical help with Appendix I and to Beatrice Golomb for comments on an earlier version of the manuscript.

References

Attneave F, 1954 "Some informational aspects of visual perception" *Psychological Review* **61** 183–193

Barlow H B, 1961 "Possible principles underlying the transformations of sensory messages" in *Sensory Communication* ed W A Rosenblith pp 217–234 (New York: John Wiley)

Barlow H B, Levick W R, 1965 "The mechanism of directional selectivity in rabbit's retina" *Journal of Physiology (London)* **178** 477 - 504

Braddick O J, 1974 "A short range process in apparent motion" *Vision Research* **14** 519 - 527

Doorn A J van, Koenderink J J, 1982 "Spatial properties of the visual detectability of moving spatial white noise" *Experimental Brain Research* **45** 189 - 195

Hubel D H, Wiesel T N, 1968 "Receptive fields, binocular interactions and functional architecture of monkey striate cortex" *Journal of Physiology (London)* **195** 215 - 243

Julesz B, 1971 *Foundations of Cyclopean Perception* (Chicago, IL: University of Chicago Press)

Koenderink J J, Doorn A J van, 1976 "The local structure of movement parallax of the plane" *Journal of the Optical Society of America* **66** 717 - 723

Lappin J S, Bell H H, 1976 "The detection of coherence in moving random-dot patterns" *Vision Research* **16** 161 - 168

Lappin J S, Fuqua M, 1982 "Non-linear recruitment in the visual detection of moving patterns" *Investigative Ophthalmology and Visual Science, Supplement* **22** 123

McKee S P, Welch L, 1982 "Sequential recruitment in the discrimination of velocity" *Journal of the Optical Society of America* **A2** 243 - 251

Meeteren A van, Barlow H B, 1981 "The statistical efficiency for detecting sinusoidal modulation at average dot density in random figures" *Vision Research* **21** 765 - 778

Mulligan J B, MacLeod D I A, 1984 "Pooling of perceived brightness among distinct texture elements" *Investigative Ophthalmology and Visual Science, Supplement* **24** 199

Nakayama K, 1981 "Differential motion hyperacuity under conditions of common image motion" *Vision Research* **21** 1475 - 1482

Nakayama K, Silverman G H, 1984 "Temporal and spatial aspects of the upper displacement limit in random dots" *Vision Research* **24** 293 - 299

Nakayama K, Tyler C W, 1978 "Relative motion induced between stationary lines" *Vision Research* **18** 1663 - 1668

Nakayama K, Tyler C W, 1981 "Psychophysical isolation of movement sensitivity by removal of familiar position cues" *Vision Research* **21** 427 - 433

Rogers B, Graham M, 1979 "Motion parallax as an independent cue for depth perception" *Perception* **8** 125 - 134

Rogers B, Graham M, 1982a "Similarities between motion parallax and stereopsis in human depth perception" *Vision Research* **22** 261 - 270

Rogers B, Graham M, 1982b "Horizontal - vertical anisotropies in the perception of 3-D depth surfaces" *Investigative Ophthalmology and Visual Science, Supplement* **22** 273

Rogers B, Graham M, 1983 "Anisotropies in the perception of three-dimensional surfaces" *Science* **221** 1409 - 1411

Tyler C W, Torres J, 1972 "Frequency response characteristics for sinusoidal movement in the fovea and periphery" *Perception & Psychophysics* **12**(2B) 232 - 236

Appendix 1. Under general conditions, a velocity field can be expressed as a superposition of sinusoidal waves of compression and shear.

In a velocity field, the velocity at each point (x, y) can be regarded as the vector sum of horizontal and vertical components. We shall use $V_x(x, y)$ and $V_y(x, y)$, respectively, to denote the signed magnitudes of these components. These magnitudes are each scalar functions of x and y. We assume they have Fourier transforms, that is that $V_x(x, y)$ and $V_y(x, y)$ are each expressible as a superposition of sine and cosine components varying in angular frequency, ω, and orientation, θ (defined here as the angle between the direction of modulation and the x axis). Thus:

$$V_x(x, y) = \int_{-\pi/2}^{\pi/2} \int_{-\infty}^{\infty} A_{xs}(\omega, \theta) \sin(\omega d_\theta) + A_{xc}(\omega, \theta) \cos(\omega d_\theta) \, d\omega \, d\theta , \qquad \text{(A1.1)}$$

where $A_{xs}(\omega, \theta)$ is the Fourier sine transform of $V_x(x, y)$ and $A_{xc}(\omega, \theta)$ is its Fourier cosine transform. [The argument d_θ which is equal to $(x\cos\theta + y\sin\theta)$ represents the component of the vector from the origin to the point (x, y) in the θ direction, figure A1.] The functions $A_{yc}(\omega, \theta)$ and $A_{ys}(\omega, \theta)$ are defined by direct analogy for the vertical velocity components.

To show that the original field may be decomposed into compression and shear components, it will now suffice to show that this may be done for any two-dimensional sinusoid of horizontal or vertical velocity, corresponding to an individual Fourier component as in equation (A1.1). The way that a sinusoidal wave of horizontal (vertical) motion can be decomposed into compression and shear waves of the same phase, orientation, and spatial frequency is shown for a wave of horizontal velocity in figure A2.

To show this algebraically, we note that we may decompose any vector into a component in the θ direction (the ascending rightward vectors in figure A2), and a component in the orthogonal direction (the descending rightward vectors in figure A2). The components in the θ direction constitute a pure compression wave, and the orthogonal components constitute a pure shear wave. If the original vector is a horizontal vector of unit magnitude, denoted as $\hat{x}$ (with $\hat{y}$ for the vertical unit vector), then the component in the θ direction will have magnitude $\cos\theta$, and the perpendicular component will have magnitude $\sin\theta$. Let $\kappa_c(\omega, \theta)$ and $\sigma_c(\omega, \theta)$ represent a cosine phase compression and shear waves, respectively, of orientation θ and frequency ω:

$$\kappa_c(\omega, \theta) = (\hat{x}\cos\theta + \hat{y}\sin\theta)\cos(\omega d_\theta) ,$$

$$\sigma_c(\omega, \theta) = (\hat{x}\sin\theta - \hat{y}\cos\theta)\cos(\omega d_\theta) .$$

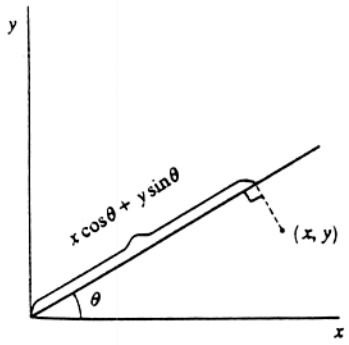

Figure A1. When a field is modulated one-dimensionally in the direction θ, the effect at a point (x, y) depends only on d_θ which we define as $(x\cos\theta + y\sin\theta)$. This is the component in the direction θ of the vector from the origin to the point (x, y) and is constant along lines perpendicular to the direction θ.

We may decompose the horizontal vector field in figure A2, which corresponds to one of the Fourier components in equation (A1.1), as follows:

$$\hat{x}\cos(\omega(x\cos\theta + y\sin\theta)) = \kappa_c(\omega, \theta)\cos\theta + \sigma_c(\omega, \theta)\sin\theta,$$

$$\hat{y}\cos(\omega(x\cos\theta + y\sin\theta)) = \kappa_c(\omega, \theta)\sin\theta - \sigma_c(\omega, \theta)\cos\theta.$$

The Fourier components for vertical motion may be decomposed into shear and compression in like fashion.

We have derived the amount of shear and compression present in a single Fourier component of horizontal or vertical motion; we now conclude by expressing the total amounts of compression and shear in the original field in terms of the Fourier transforms of the magnitudes of the horizontal and vertical components. The amplitude of the cosine phase compression wave with parameters ω, θ, denoted by $A_{\kappa_c}(\omega, \theta)$, is the sum of two terms, one due to the horizontal velocity component, the other to the vertical:

$$A_{\kappa_c}(\omega, \theta) = A_{xc}(\omega, \theta)\cos\theta + A_{yc}(\omega, \theta)\sin\theta.$$

Similarly for shear:

$$A_{\sigma_c}(\omega, \theta) = A_{xc}(\omega, \theta)\sin\theta - A_{yc}(\omega, \theta)\cos\theta.$$

Similar expressions may be written to describe the sine phase components.

The preceding discussion may have left the impression that these shear and compression waves are adequate to describe any velocity field. This is not strictly true. Two simple examples of vector fields for which the x and y component magnitudes do not have Fourier transforms are rigid rotation of the whole visual field, and uniform dilation of the field about a point or a line. In both cases, difficulty arises because the velocities become unbounded.

One more complex vector field exists which partakes neither of shear nor of compression. These fields are sometimes called 'deformation fields' (Koenderink and van Doorn 1976). The general form of these fields is one with a stationary point with radiating spokes alternating between inflow and outflow, with velocities going to infinity so that there is no Fourier transform.

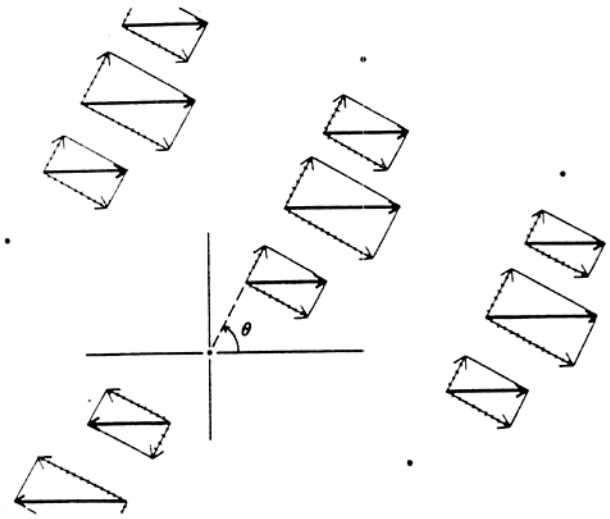

Figure A2. Heavy lines show a sine wave of horizontal velocity, modulated in the direction θ. Hatched lines show how it can be decomposed into a compression component (hatched vectors ascending rightward) and a shear component (hatched vectors descending rightward). The two sine-wave components are similar in phase, spatial frequency, and direction of modulation θ, but their velocity vectors are at right angles everywhere.